Metalloporphyrins in Prebiotic Photocatalysis and Bioenergetics

A Thesis

submitted to

Indian Institute of Science Education and Research Pune in partial fulfilment of the requirements for the BS-MS Dual Degree Programme

by

G V Anuraag Aithal

Indian Institute of Science Education and Research Pune

Dr. Homi Bhabha Road,
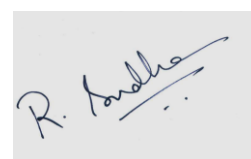
Pashan, Pune 411008, INDIA.

April, 2023

Supervisor: Dr. Sudha Rajamani

Your Name: G V Anuraag Aithal

Certificate

This is to certify that this dissertation entitled Metalloporphyrins in Prebiotic Photocatalysis and Bioenergetics towards the partial fulfilment of the BS-MS dual degree programme at the Indian Institute of Science Education and Research, Pune represents study/work carried out by G V Anuraag Aithal at Indian Institute of Science Education and Research under the supervision of Dr. Sudha Rajamani, Associate Professor, Department of Biology, during the academic year 2022-2023.

Dr. Sudha Rajamani

Committee:

Name of your Guide: Dr. Sudha Rajamani

Name of Your TAC: Dr. V. G. Anand

Dedicated to everyone from whom I have learnt, in science and in life, for they have helped me grow, made me a better scientist and a better human.

Declaration

I hereby declare that the matter embodied in the report entitled Metalloporphyrins in Prebiotic Photocatalysis and Bioenergetics are the results of the work carried out by me at the Department of Biology, Indian Institute of Science Education and Research, Pune, under the supervision of Dr. Sudha Rajamani and the same has not been submitted elsewhere for any other degree

Your Name: G. V. Anuraag Aithal

Date: March 31st, 2023

Table of Contents

List of Figures

Abstract

Metalloporphyrins are widespread in the bioenergetics of extant biology and are plausible candidates for similar roles during the origins of life. Sunlight is the source of energy for the vast majority of the extant biosphere and could have driven reactions of interest to origins of life. However, selectivity in such reactions requires catalytic intervention. Towards this, we investigate the plausible role the porphyrin macrocycles and corresponding metalloporphyrins could have played as photocatalysts in the origins of life. We compare the photocatalytic performance of the different metalloporphyrins through various model reactions and try to rationalise the selection of the Mg^{2+}-complex in extant biology. It is observed that only a subset among the porphyrin macrocycle and the metalloporphyrins are photocatalytically viable. Mechanistic investigations point towards the role of stable excited states in enabling photocatalytic properties. This sets the stage towards studying reactions of very direct relevance to prebiotic chemistry, in order to understand the kind of processes that could have been photocatalytically driven on the prebiotic earth.

Acknowledgments

I am thankful to Dr. Sudha Rajamani, my thesis supervisor, for her motivation and support throughout the project, and allowing me to be creative throughout. My thanks to the members of the COoL Lab – particularly, Shikha Dagar and Anupam Sawant, who have mentored me during the project. My thanks to my TAC member Dr. V. G. Anand for his meaningful inputs and allowing me to work with his lab resources, as also his lab members who have helped in many reactions.

I thank Dr. Amrita Hazra and her lab members for allowing the use of the glove bag. I thank Dr. Pramod Pillai and his lab members, particularly Vanshika Jain and Indranarayan Chakraborty for their inputs and guidance, as well as the help in the fluorescence lifetime experiments.

Most importantly, to my friends and family, who have been my safe-space and a source of inspiration to constantly grow as a human, I am immensely grateful.

Chapter 1 **Contributions**

Contributor name	Contributor role
G V Anuraag Aithal Shikha Dagar Dr. Sudha Rajamani	Conceptualization Ideas
G V Anuraag Aithal Dr. Sudha Rajamani	Methodology
-	Software
Dr. Sudha Rajamani	Validation
G V Anuraag Aithal	Formal analysis
G V Anuraag Aithal	Investigation
Dr. Sudha Rajamani	Resources
G V Anuraag Aithal	Data Curation
G V Anuraag Aithal	Writing - original draft preparation
Dr. Sudha Rajamani	Writing - review and editing
G V Anuraag Aithal	Visualization
Dr. Sudha Rajamani	Supervision
Dr. Sudha Rajamani	Project administration
Dr. Sudha Rajamani	Funding acquisition

Chapter 2 Introduction

"But if (and oh what a big if) we could conceive in some warm little pond with all sort of ammonia and phosphoric salts,—light, heat, electricity present, that a protein compound was chemically formed, ready to undergo still more complex changes, at the present such matter would be instantly devoured, or absorbed, which would not have been the case before living creatures were formed"

-Charles Darwin in his letter to Joseph Dalton Hooker, dated February 1st, 1871.

The works of Darwin, Malthus and co. took the explanation about the diversity of life forms out of the realm of the divine and gave, for the first time, the possibility of systematically answering these questions using pertinent scientific tools. The currently accepted theory for the origins of biodiversity suggests that life diversified due to descent with modification, with reproductive fitness acting as the leading force for the selection of new life forms (Herron et al., 2015).

However, this left scientists still wondering regarding the first forms of life and how it came into existence. Darwin's warm little pond speculation (in a letter to Hooker) suggested that biomolecules may have first formed in prebiotic oceans and lakes before undergoing evolution into more complex forms. Yet, it took more than half a century before a reasonably concrete hypothesis was formulated by A. I. Oparin and Haldane. And it took nearly hundred years for the first experimental proof to arrive when Stanley Miller demonstrated the formation of biomolecules in simulated prebiotic Earth conditions (Miller, 1953). Experimental demonstrations thereafter focussed for a long time on the generation of the different biomolecular classes in simulated prebiotic Earth conditions. Such experiments, however, overlooked how this might fit into an evolutionary pathway towards the life as we know it. Detailed understanding of biochemistry and molecular biology brought the realisation that there is more to life than thinking about it as collection of biomolecules. It is a self-organised system with a definite pattern in its spatio-temporal and functional organisation (Smith & Morowitz, 2016). Therefore, it has been argued that origins of life should be studied accounting for the emergence and sustenance of such physico-chemically ordered systems.

In particular, all life forms consist of three hallmark features: the genetic machinery, the cellular architecture and the metabolic network. The universality of these features

suggests that these were an integral part of the earliest life forms. And, given their centrality to all life we know, it is reasonable to assume that these were the earliest components of life to have emerged during the transition from non-life to life on the early Earth. The leading hypotheses for the origins of life explore the possibility of one of these characteristics having emerged prior, and supporting the emergence of the other features of life. The genetic machinery in extant biology is involved in the transfer of information within a cell as well as transfer across generations (Alberts et al., 2017). The simultaneous capability of RNA to carry information and perform catalysis allowed conceptually simplifying the origins of a genetic machinery during the origins of life to a self-replicating RNA (Robertson & Joyce, 2012). Given this, the formation of functionally active polymers and the demonstration of self-replicating functions have been the thematic questions for the "RNA World" hypothesis. As is evident from extant life, the genetic machinery is among the central components of an extensively interdependent network that sustains life. The well-defined interactions among these components are possible due to the cellular nature that (among other functions) defines spatial proximity for the network components. This makes compartmentalisation another fundamental target for origins life research (Sarkar et al., 2020). Various model compartments have been proposed and studied in this context, ranging mainly from homogenous vesicles to, more recently, complex droplets and coacervates.

While the membranes and the encapsulated genetic material are among the major components of living organisms, equally important are the processes required to generate and sustain the chemical systems. All living organisms are steady-state, out-of-equilibrium systems and they are maintained in this state by the underlying metabolic network (Branscomb & Russell, 2018; Smith & Morowitz, 2016). For e.g., extant biochemistry works to maintain homeostasis in the concentrations and compositions of biomolecules, relying on a defined set of substrates, intermediates and pathways (Branscomb & Russell, 2018). However, the abiotic environment by itself does not produce these metabolites – rather it furnishes the elements in inorganic forms like CO_2, N_2, etc. Autotrophs harness energy from the environment to convert these inputs into appropriate metabolites. A continuous input of energy is therefore necessary to keep living systems in the out-of-equilibrium state, and therefore, keep them alive.

This lays foundation for the thematic question in prebiotic chemistry that needs to be addressed: The early Earth furnished the necessary inorganic inputs like CO_2, NH_3, etc. Starting with these molecules, what processes would have led to the formation of biomolecules like α-keto acids, sugars, amino acids, etc?

By definition, the majority of such transformations in extant biology are redox reactions (Smith & Morowitz, 2016). On the early Earth, there were two primary sources of energy to drive biosynthesis through such redox reactions: sunlight and geochemical redox gradients. Geochemical redox gradients, such as those present in submarine hydrothermal vents, have been shown to be capable of extensive carbon fixation, leading to the formation of important biosynthetic intermediates (Muchowska et al., 2020; Preiner et al., 2020; Varma et al., 2018). These environments are particularly favourable for generation of reduced carbon substrates since the extremely reducing environments favour carbon fixation starting from CO_2. Interestingly, the free energy alone does not suffice for carbon fixation and these reactions only proceed with catalytic assistance from the minerals present in these niches (Muchowska et al., 2020). These catalyst minerals, which are almost invariably iron-containing, bear semblance to metal centres of extant metalloenzymes, particularly iron-sulfur clusters (Preiner et al., 2020). The other important source of energy for life's origins could be sunlight, which in extant biology provides energy for most of carbon fixation. Because of its ready availability as a source of energy during the origins of life, it is intuitive to consider the role it might have played in this process. Light dependent reactions of interest to origins of life have been experimentally demonstrated earlier (Bonfio et al., 2017; Green et al., 2021; D. J. Ritson et al., 2020; D. Ritson & Sutherland, 2012). But in the absence of a catalyst, photochemistry can be fairly non-selective. Alternatively, a photocatalyst can, in principle, drive selective endergonic redox reactions. From the perspective of prebiotic chemistry, this could have led to the synthesis of biomolecules on the prebiotic Earth, possibly leading to increasing complexity in the biomolecular inventory and the reaction networks.

Given the aforesaid, dedicated systems are necessary in either cases to harness energy from the environment and drive selective transformations, which are normally inaccessible due to thermodynamic or kinetic barriers. In extant biology, the functions of bioenergetics belong exclusively to sophisticated proteins. The light-harvesting complex obtains energy from sunlight whereas hydrogenases receive

reducing electrons from hydrogen for reduction of various substrates. However, the sequence-specificity along with the size of the protein polymers suggest that proteins are products of life and are not ideal candidates for consideration in the bioenergetics relevant to life's origins. Importantly, the enzymes involved in bioenergetics are predominantly metalloenzymes, with a metal-containing cofactor being at the functional centre (Smith & Morowitz, 2016). This allows to envisage a simpler scenario for the origins of bioenergetics, where the metal-containing cofactors performed similar functions before proteins arose. These were potentially later scaffolded, first by short peptides and later by proteins themselves, once a proto-translational system and a more elaborate energy conservation mechanism was in place (Dagar et al., 2022).

Cofactors being relatively simpler in architecture, are more likely to have been present on the prebiotic Earth. These are function-specific but not as substrate-specific as enzymes. This property allows reusing a given cofactor for a large set of substrates undergoing similar transformations, or for fundamentally similar processes in different pathways. In the context of prebiotic chemistry, this promiscuity, in principle, could have allowed a small set of cofactors to lead to an extensive diversification of synthetic pathways. The question then is, which cofactors do we consider for bioenergetics? Protein evolution has shown convincingly that iron-sulfur clusters have the most ancient protein folds, which later evolved into heme and other oxidoreductase enzymes (Bromberg et al., 2022; Harel et al., 2014; Raanan et al., 2018). These cofactors are predominantly involved in electron transfer reactions for a diverse set of pathways, including the fixation of elements into organic molecules. Phylometabolic analysis of biosynthetic pathways further supports the idea of iron-sulfur clusters being catalysts in possibly the most ancient carbon-fixation pathways, which further supports their antiquity in bioenergetics. The other prominent class of cofactors involved in bioenergetics are the porphyrin-complexes. Porphyrins are ubiquitous in biology, manifesting in a wide variety of functions by complexing (the various derivatives) with different metal ions. These include electron transfers performed by the complex containing Fe^{2+}/Fe^{3+}, radical reactions through the cobalt-corrin complex, methyl group transfer via the Ni^{2+}-containing F430 in the acetyl-CoA pathway (considered to be among the first protometabolic pathways), to name a few. Of particular relevance in bioenergetics is the Mg^{2+}-chlorin complex, known as chlorophyll. This complex absorbs sunlight and transfers the excited state

electrons, leading to the generation of high energy molecules like NADH and the biosynthesis of sugars.

Experiments in prebiotic chemistry have demonstrated the possibility of forming porphyrin macrocycles (Simionescu et al., 1978) and subsequently metalloporphyrins on the prebiotic Earth (particularly the complexes of Mn^{2+}, Co^{2+}, Ni^{2+}, Cu^{2+} and Zn^{2+}(Dagar et al., 2022)). Previous experiments have also demonstrated that some of the metal-porphyrin complexes and the porphyrin macrocycle (without an enzymatic machinery) itself are photocatalytically active (Soares et al., 2012). This suggests that simple cofactors, sans enzymes, could have been photocatalysts during the origins of life. Nevertheless, this activity has not been systematically assessed for the complexes with the entire set of biologically relevant metal ions. The possibility of alternate metalloporphyrins having functioned as prebiotic photocatalysts has also not been considered thus far. This is relevant as prebiotic niches would have consisted of a diversity of metal ions, which could have complexed with porphyrin macrocycles and formed metalloporphyrins, potentially leading to a repertoire of functions as in extant biology. Furthermore, we do not have a rigorous understanding of what partitions different metalloporphyrin complexes into distinct roles – specifically in this case, what selection pressures brought Mg^{2+}-chlorin complex into the exclusive role in light harvesting. Finally, it is not well understood what kind of processes of interest to origins of life could have been driven by such metalloporphyrins.

In this thesis, we aimed to obtain robust conclusions about the photocatalytic activity of metalloporphyrins, while also attempting to understand in terms of molecular properties any resulting differences therein. Specifically, we worked with the metalloporphyrins of Mg^{2+}, Mn^{2+}, Co^{2+}, Ni^{2+}, Cu^{2+} and Zn^{2+}. Geochemical records indicate the clear abundance of some of these metal ions in the Archaean Ocean, but some others were chosen due to their relevance to extant biology. A few selection pressures were assessed to answer regarding the possible role of metalloporphyrins as prebiotic photocatalysts. We also try to investigate if the prebiotic repertoire of photocatalysts could have been different from the photocatalyst in extant biology. Finally, we aimed to demonstrate the capability of these metalloporphyrins in driving endergonic reactions of interest to origins of life.

Chapter 3 Materials and Methods

1. Synthesis of metal-TPPS complexes

TPPS (meso-tetra-(4-sulfonatophenyl) porphyrin) was used as a porphyrin derivative in most experiments, unless otherwise mentioned. The presence of four ionisable groups, allows solubilising an otherwise hydrophobic porphyrin macrocycle in water. TPPS was procured from Sigma Aldrich and used without further purification. A modification of the previously reported procedure (Dagar et al., 2022) was used for the synthesis of the metal complexes (see Figure 1). Briefly, 500 µM TPPS was incubated with 1.5 mM of the metal-sulfate salt and 3 mM NaOH at 80°C. The complete formation of the metalated complexes could be inferred from the change in the absorbance spectra. The intense Soret-band (centred at 413 nm) for TPPS shifts to either higher (for Mn^{2+}-TPPS, Co^{2+}-TPPS, Zn^{2+}-TPPS) or lower wavelengths (Ni^{2+}-TPPS and Cu^{2+}-TPPS). Since the Soret-bands of most of the metalloporphyrins overlap with TPPS, the shift in Soret-band maxima cannot be confirmatory for metalation reactions. A more confirmatory signature is the reduction in the number of Q-bands from four in TPPS to two or one in the metal complexes.
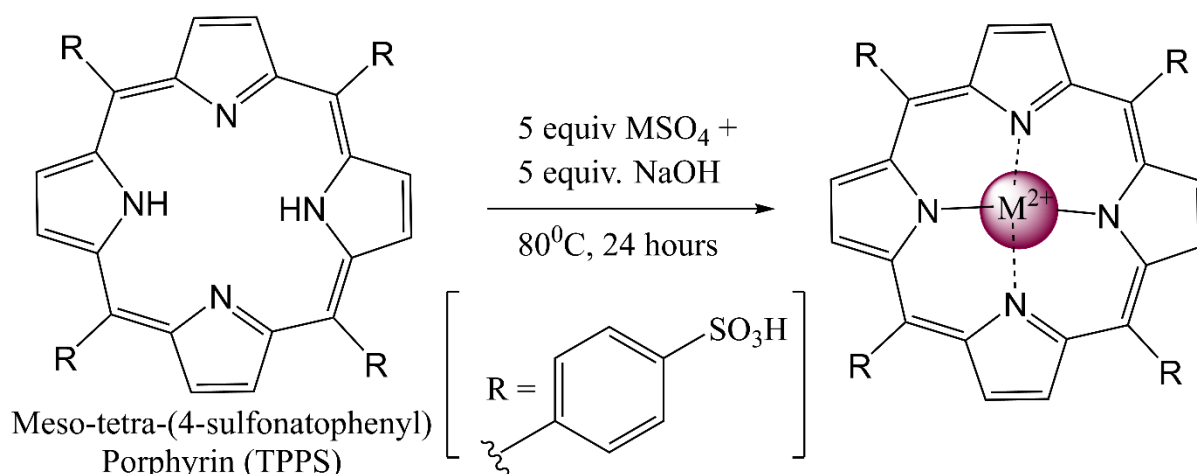

Figure 1: Schematic showing the procedure for metalation of TPPS. Briefly, TPPS is incubated with the corresponding metal sulfate salt and NaOH (to neutralise the acid groups and facilitate the deprotonation of the inner ring amine groups). This procedure allows complete metalation with Mn^{2+}, Co^{2+}, Ni^{2+}, Cu^{2+} and Zn^{2+}, all requiring varying times of incubation. However, a prolonged incubation of 2 hours was used as a safe measure to ensure the completion of the reaction.

Removal of the excess metal salts were attempted using ethanol extraction and purification using dialysis membranes. However, either method did not give satisfactory results. Instead, it was noticed that the addition of excess NaOH caused precipitation of the unreacted salts in the reaction mixture. Centrifugation of the reaction mixture or stock solutions led to the precipitation of the excess metal salts, after which the supernatant was used in the photocatalysis reactions.

While the majority of the metalation reactions went to completion, Mg^{2+}-TPPS formation saturated at around 70% despite attempting a few different protocols. Therefore, the photocatalysis data presented throughout for Mg^{2+} reactions come from a mixture of Mg^{2+}-TPPS and TPPS. In literature, this complex is generally synthesised by refluxing with a magnesium halide salt in DMF but this method did not work well in our hands. We are attempting to better understand this synthesis method or possible purification methods to obtain pure Mg^{2+}-TPPS for a more rigorous characterisation.

2. Synthesis of Tetra-(4-N-methylpyridyl) porphyrin (TMPyP)

TMPyP was used as an alternative to TPPS where the negative charge on TPPS caused precipitation with substrates. Due to the presence of four positively charged groups on the meso-positions, TMPyP is also water-soluble.

Tetrapyridyl Porphyrin (TPyP)   Tetra (4-N-methylpyridyl) Porphyrin (TMPyP)
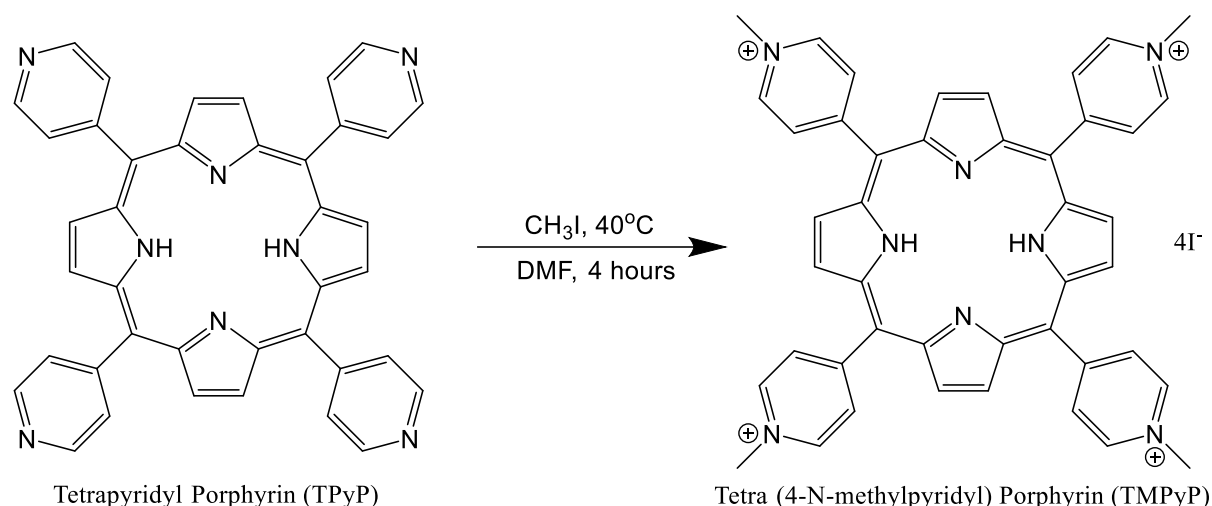
Figure 2: Procedure for the methylation of TPyP (left) into TMPyP (right). Briefly, the procedure involved the reaction of TPyP with excess iodomethane in DMF, at 40°C, followed by solvent removal and crystallisation of the product.

Tetra pyridyl porphyrin (TPyP) and Iodomethane were purchased from TCI chemicals and Spectrochem, respectively, and used without further purification. The synthesis of Tetra-(4-N-methylpyridyl) porphyrin iodide (TMPyP) was done based on the previously reported procedure. Briefly, 27mg of TPyP and 1.215 mL of iodomethane were reacted in 4 mL N, N-DMF at 40^0 C (Figure 2). The reaction was monitored through normal phase TLC using a 20:80 MeOH: DCM mixture. While the reported procedure suggested keeping the reaction for 24 hours, the reactant spot could not be seen after 2 hours so the reaction was quenched after 4 hours to avoid any possible parasitic reactions.
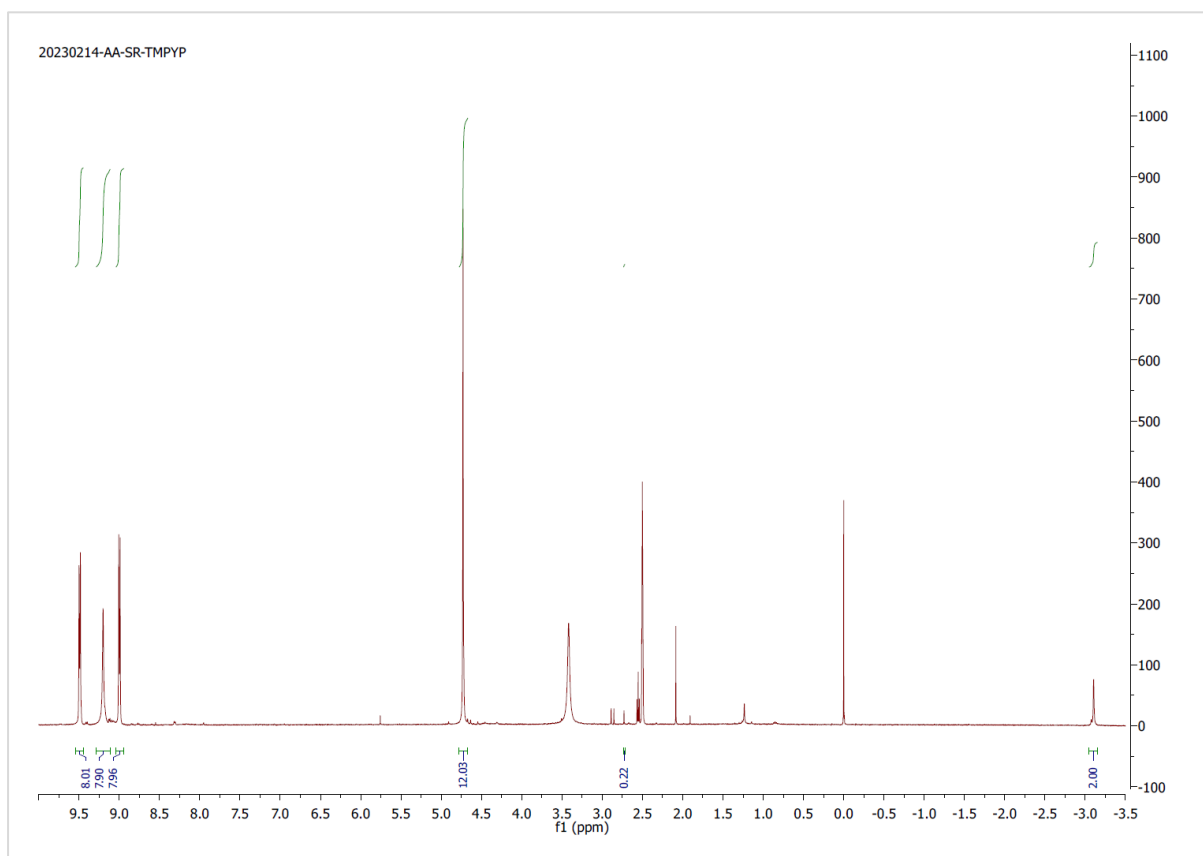

Figure 3: 1H NMR spectra used for the confirmation of the methylated derivative, TMPyP, recorded in DMSO-d6. The two inner ring protons have signals at -3.11 ppm, as reported previously, whereas for the starting material TPyP, the corresponding signals appear at 2.99 ppm. The singlet at ~4.75 ppm corresponds to the 12 protons on the 4 methyl groups (in methyl-pyridyl substituent). The three peaks between 9.0 and 9.5 ppm correspond to the eight each of β, o- and m-protons. The unlabelled heptet at 2.5 ppm corresponds to the protons in solvent and the singlet at ~3.5 due to residual H_2O in the solvent.

Thereafter, DMF was removed under reduced pressure by mixing with toluene to lower the boiling point. The resulting solid was crystallised in MeOH: EtOAc to yield

the desired product. The product was confirmed through 1H-NMR (Figure 3) and HRMS analysis. Due to multiple fragmentation patterns, however, HRMS could not yield clear results. IN 1H-NMR (in DMSO-d6) the appearance of the inner ring proton signals at 3.11 ppm and disappearance at 2.99 ppm confirmed the completion of the reaction.

3. Methyl Red Photoreduction assay

Methyl Red was used as is from Sigma Aldrich. The stock was prepared by first adding concentrated NaOH to it (in approx. equimolar quantities) and then dissolving the resulting methyl red sodium salt in water. The exact concentration was then determined using UV-Visible spectrophotometry (ε = 23360/M-cm at 429 nm).

The photoreduction assay(Soares et al., 2012) consisted of 50 µM methyl red in 100 mM (Na-)phosphate buffer adjusted to pH ~7.2. 1 mM ascorbic acid was used the sacrificial electron donor, along with 500 nM (0.5 µM) TPPS or the relevant metal-TPPS complex as the photocatalyst candidate. The reaction was set up inside an anaerobic chamber with [O_2] between 130-140 ppm. Anoxygenic environment is necessary to ensure the progress of the reaction as well as to ensure that some of the complexes (particularly Mg^{2+}-TPPS and Zn^{2+}-TPPS) do not undergo photobleaching.

The reaction mixture was sealed inside the glove bag and then illuminated using a 100W Phillips halogen UV-open lamp for 5 minutes. The temperature could not be controlled or monitored during the reaction, but the illumination times were kept short in order to prevent warming of the reaction mixture. Nevertheless, any background reactivity that might happen due to temperature changes would be accounted for by the control reaction that was also setup in a similar manner.

The absorbance spectra were recorded for aliquots taken before and after the illumination (T = 0 mins and T = 5 mins). The reduction product, leuco-methyl red, is colourless and does not absorb in the visible region. The reaction progress, then, is assayed using the absorbance values at 440 nm:

[Methyl Red reduced (µM)] = 100 * [A(440, T=0) - A(440, T=5)] / [2 * A(440, T=0)]

wherein A440 in the absorbance at 440 nm for the aliquot taken at the time mentioned within the parentheses. The value was chosen at 440 nm instead of 429

nm because at 429 nm, there is contribution from both methyl red and the metalloporphyrins/TPPS. For Mg^{2+}-TPPS, the quantification was done at 450 nm since it shows overlap at both 429 nm and 440 nm. The absorbance measurements for UV-visible spectroscopy were performed on Shimadzu UV-1800 double beam spectrophotometer using a cuvette of path length 10 mm. In this experiment, 100 mM phosphate buffer was used as the reference solution since this was the background medium for the reaction setup as well.
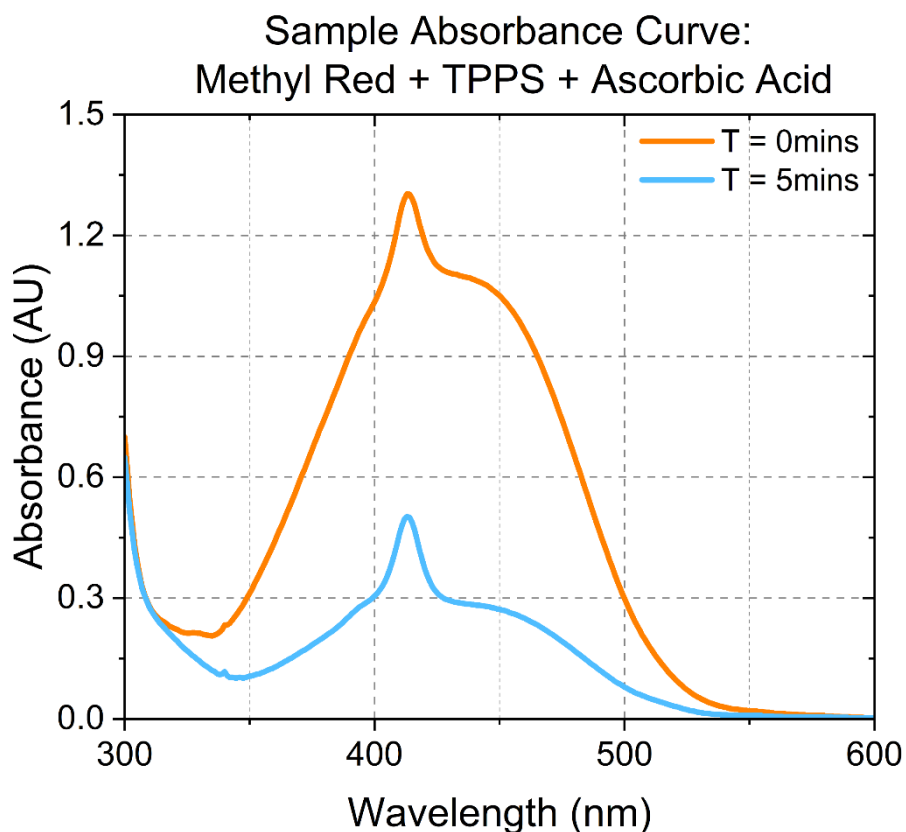

Figure 4: A representative absorbance spectra depicting the analysis method. Methyl red has an absorbance maximum at 429 nm, but since the porphyrins also absorb at this wavelength, the absorbance at 440 nm is used for quantification. The reduction product, leuco-methyl red does not absorb in this wavelength range. The absorbance values are therefore used to track the extent of reaction in 10 mins.

A drawback of this methodology is, however, that due to the overlap between the spectra for methyl red and the metal-TPPS complexes, it is hard to rigorously keep track of any change in the catalyst concentration over time. Towards this, we are attempting to set up a HPLC analysis protocol to allow for separating out clearly the

methyl red, leuco-methyl red and the porphyrin complexes. If we can set up such a protocol, this will then be used to simultaneously keep track of the reaction progress and catalyst concentration during the experiment.

4. Dichlorophenolindophenol (DCPIP) photoreduction assay

DCPIP sodium salt (obtained from Sigma Aldrich) was dissolved in water to make the stock solution, and the concentration was determined using the absorbance value at 600 nm (μ = 21000/M-cm). Due to solubility and degradation issues, the stock concentrations were kept ~2-5 mM and used within a few days of preparation.

The photoreduction assay was performed using 50 µM DCPIP in 200 mM triethanolamine (TEOA) buffer adjusted to pH 7.25. Note that TEOA served as both the buffer and the sacrificial electron donor. In the experiments for the relative photocatalytic activity, the concentration of TPPS or M^{2+}-TPPS was maintained at 2.5 µM. Once set up, a typical reaction mixture was sealed and then purged with nitrogen gas for 30 minutes to create an anoxic condition for the photocatalysis experiment. The reaction mixture was illuminated using the same 100W Phillips halogen UV-open lamp for 10 minutes. The temperature could not be controlled or monitored during the reaction, but the illumination times were kept short in order to prevent warming of the reaction mixture. Nevertheless, any background reactivity stemming from temperature changes would be accounted for by the control setup. Aliquots were taken before and after the illumination and the absorbance spectra were recorded.

The extent of the reaction, calculated as the change in concentration of DCPIP after illumination is calculated as:

[DCPIP change in µM] = [A (600 nm, T = 0 mins) - A (600 nm, T = 10mins)] / 0.021

The absorbance measurements for UV-visible spectroscopy were performed on Shimadzu UV-1800 double beam spectrophotometer using a cuvette of path length 10 mm. In this experiment, 200 mM TEOA buffer was used as the reference solution since this was the background medium for the reaction setup as well.

The advantage in this case is the fact that there is no significant overlap between the absorbance spectra of DCPIP and the metal-porphyrin complexes. Hence, the extent

of the photoreduction and any possible photodegradation of the complex can be distinctly monitored on UV-visible absorbance spectroscopy using the same sample.

5. Fluorescence Spectroscopy

The fluorescence emission and excitation for the complexes were recorded on Horiba Fluoromax-4+ with a cuvette of path length of 3 mm. The slit width was kept at 1 nm for the excitation slit and 0.5 nm for the emission slit. All the complexes were excited at their respective maxima in the Soret bands and the Q bands, and the emission spectrum recorded between 400-800 nm. The samples were prepared in a 10 mM CHES buffer (adjusted to pH 9.2).

The fluorescence spectra in presence of methyl red were recorded in 10 mM phosphate buffer adjusted to pH 7.2, with slit widths of 1 nm (excitation) and 1 nm (emission); in presence of DCPIP in 200 mM TEOA buffer adjusted to pH 7.25, with slit widths of 1 nm (excitation) and 0.5 nm (emission).

6. Fluorescence Lifetime measurement:

The fluorescence lifetime was measured using a Horiba DeltaFlex Time Resolved Single Photon Counting (TCSPC) instrument. Samples were prepared in 10 mM CHES buffer adjusted to pH 9.2. Samples were excited at 405 nm using a laser of such wavelength, and emission was recorded at 641 nm (TPPS), 608 nm (Mg^{2+}-TPPS) and 604 nm (Zn^{2+}-TPPS). A weakly-scattering solution of milk powder was used to determine the IRF (Instrument Response Factor). A single-exponential decay model provided the best fit in all cases and this model-fit was used to determine the lifetime for fluorescence decay.

Chapter 4 Results and Discussion

1. Model Reactions: Relative photocatalytic performance of different metal-porphyrin complexes

We began by comparing the photocatalytic performance of the porphyrin macrocycle and the metal porphyrin complexes of Mn^{2+}, Co^{2+}, Ni^{2+}, Cu^{2+} and Zn^{2+}. This was done using multiple model reactions wherein, the porphyrin complex, if photocatalytically active, would transfer electrons from an electron donor to an acceptor under illumination. Here, the choice of substrates may not necessarily have direct relevance to substrates and reactions of interest to prebiotic chemistry. Nevertheless, through the use of different electron donor-acceptor pairs, we can infer whether a porphyrin complex is photocatalytically active, and if so, with different substrates.

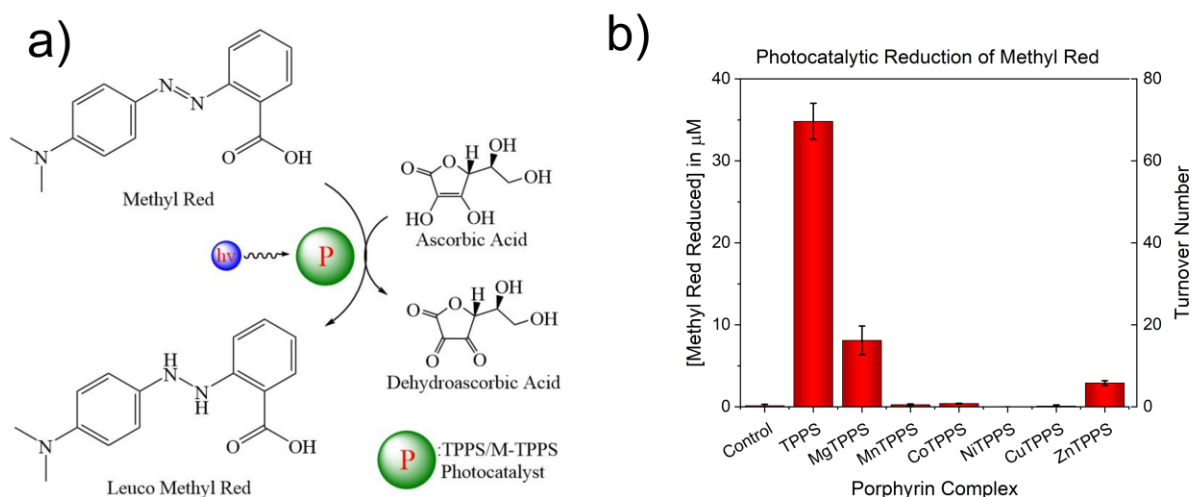*1.1.   Photoreduction of methyl red with ascorbic acid*

Figure 5: (a) Schematic depicting the photoreduction of methyl red using ascorbic acid, with the photocatalyst in presence of light. Methyl red is reduced into leuco-methyl red. (b) Extent of reduction of methyl red in the control setup and with the various metalloporphyrins. The data is the average of two replicates and error bars are standard deviations.

We first studied the photoreduction of methyl red (into leuco-methyl red) using electrons from ascorbic acid (Figure 5 (a)). Methyl red consists of a diazo-group which can undergo reduction into an -NH-NH- functional group. The reaction, termed in the literature as the *Krasnovsky reaction*, was previously reported for different porphyrin macrocycle derivatives. In previous literature (Soares et al., 2012), pre-reduced dichlorophenolindophenol (DCPIP) was used as an electron donor. It was generated using an excess of ascorbic acid added to a setup containing methyl red, DCPIP and the various porphyrin derivatives. We used a simpler version of this reaction where no electron mediator (DCPIP) was used so that there is direct electron transfer from ascorbic acid to methyl red via the photocatalyst.

Under illumination for five minutes, with 500 nM of porphyrin macrocycle/metal complex (100:1 ratio for substrate: catalyst), TPPS reduces about 35 µM of methyl red, whereas Mg^{2+}-TPPS and Zn^{2+}-TPPS reduced about 8 µM and 3.5 µM respectively (Figure 5 (b)). Compared to the control reaction, the extent of photoreduction is not significantly different in case of Mn^{2+}-TPPS, Co^{2+}-TPPS, Ni^{2+}-TPPS and Cu^{2+}-TPPS. The control setup essentially consisted of only the dye and ascorbic acid in the buffered medium, illuminated for five minutes. Additional control experiments were performed for the cases with TPPS, Mg^{2+}-TPPS and Zn^{2+}-TPPS to ascertain the nature of the reactions. Organic dyes are often prone to photodegradation instead of photoredox and to eliminate this possibility, similar reactions were setup without ascorbic acid. In all such experiments, there was no detectable quantitative change in the substrate methyl red after illumination. This confirmed the photoredox nature of the reactions in all cases.

A defining feature of catalysts is that they remain unchanged after a reaction cycle, so that they are available for the next round of catalysis. Due to the overlap between the absorbance spectra of methyl red and the porphyrin complexes, the stability of the catalysts over the course of illumination could not be quantified. Nevertheless, the high turnover numbers (~65 for TPPS, ~15 for Mg^{2+}-TPPS and ~7 for Zn^{2+}-TPPS) suggest that the photocatalysts do not get consumed during the reaction, and are acting as catalysts for electron transfers.

In future, these experiments will be possibly repeated with HPLC-based separation and analysis to quantify the stability of the photocatalysts.

1.2. Photoreduction of DCPIP with triethanolamine (TEOA)

We next looked at the photoreduction of dichlorophenolindophenol (DCPIP). DCPIP has two aromatic rings bridged by an imine ($-N=C_{aromatic}$) group with the reduction converting the blue coloured DCPIP into a colourless leuco-DCPIP, wherein the ketone group is reduced to an alcohol group. Thus, in terms of the functional groups, this would bear semblance to the reduction of Ubiquinone to Ubiquinol, a process central to the electron transport chain of photosynthesis and respiration. 200 mM Triethanolamine (TEOA) adjusted to pH 7.25 served as the electron donor (and buffer) for the reaction (Figure 6 (a)).
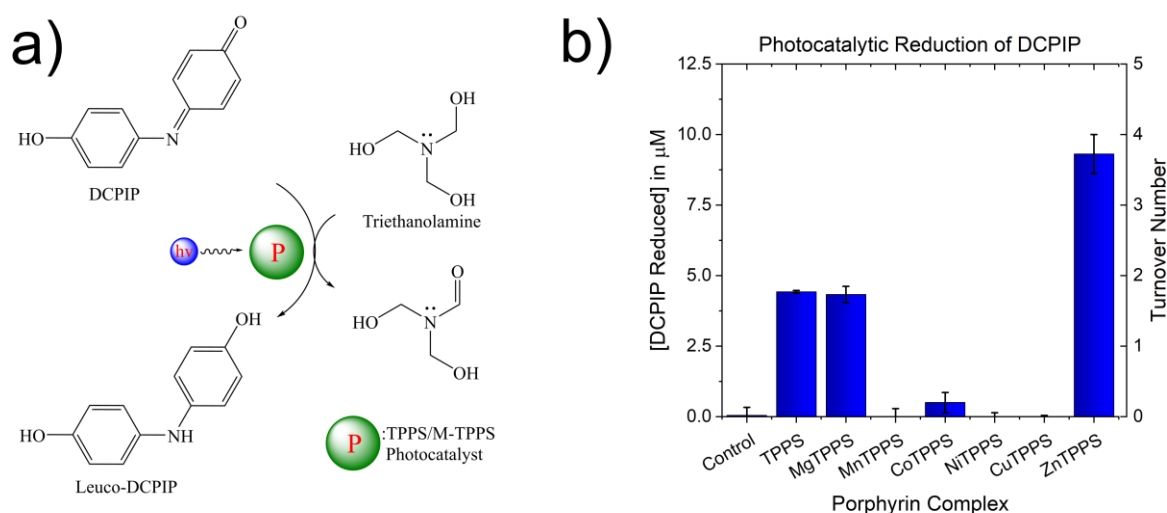

Figure 6: (a) Schematic depicting the photoreduction of DCPIP using triethanolamine, with the photocatalyst, in presence of light. DCPIP, blue in colour is reduced into the colourless leuco-DCPIP. (b) Extent of reduction of DCPIP in the control setup and with the various metalloporphyrins. The data is the average of two replicates and error bars are standard deviations. Note that while TPPS, Mg^{2+}-TPPS and Zn^{2+}-TPPS are photocatalytically active as in the previous experiment, the quantitative trends are different.

The photocatalysis experiment involved 2.5 μM of the porphyrin complexes (20:1 ratio for substrate: catalyst) and ten minutes of illumination. TPPS, Mg^{2+}-TPPS and Zn^{2+}-TPPS showed significantly higher photoreduction of DCPIP compared to the control experiment that consisted of illuminating the dye in TEOA buffer. These led to a reduction of ~4.42, ~4.33 and ~9.31 μM DCPIP over ten minutes (Figure 6 (b)).

The photoreduction of DCPIP in the control setup is relatively negligible, and is not different from this control setup when the photocatalyst used is Mn^{2+}-TPPS, Co^{2+}-TPPS, Ni^{2+}-TPPS or Cu^{2+}-TPPS.

An important observation is that while the same porphyrin complexes are photocatalytically active with the methyl red/ascorbic acid setup presented previously and DCPIP/TEOA setup, the relative photocatalytic activities are very different. TPPS far outcompeted Zn^{2+}-TPPS and Mg^{2+}-TPPS in the methyl red photoreduction whereas Zn^{2+}-TPPS outcompetes the other two in the DCPIP photoreduction, with TPPS seeming comparable to Mg^{2+}-TPPS. Some preliminary experiments to better understand these differences are reported later.

The nature of the reactions was ascertained to be photoreduction (and not photodegradation) by replacing TEOA buffer with phosphate buffer, depriving the reaction of its electron donor. In all cases, the absorbance readout for DCPIP did not change over ten minutes of illumination.
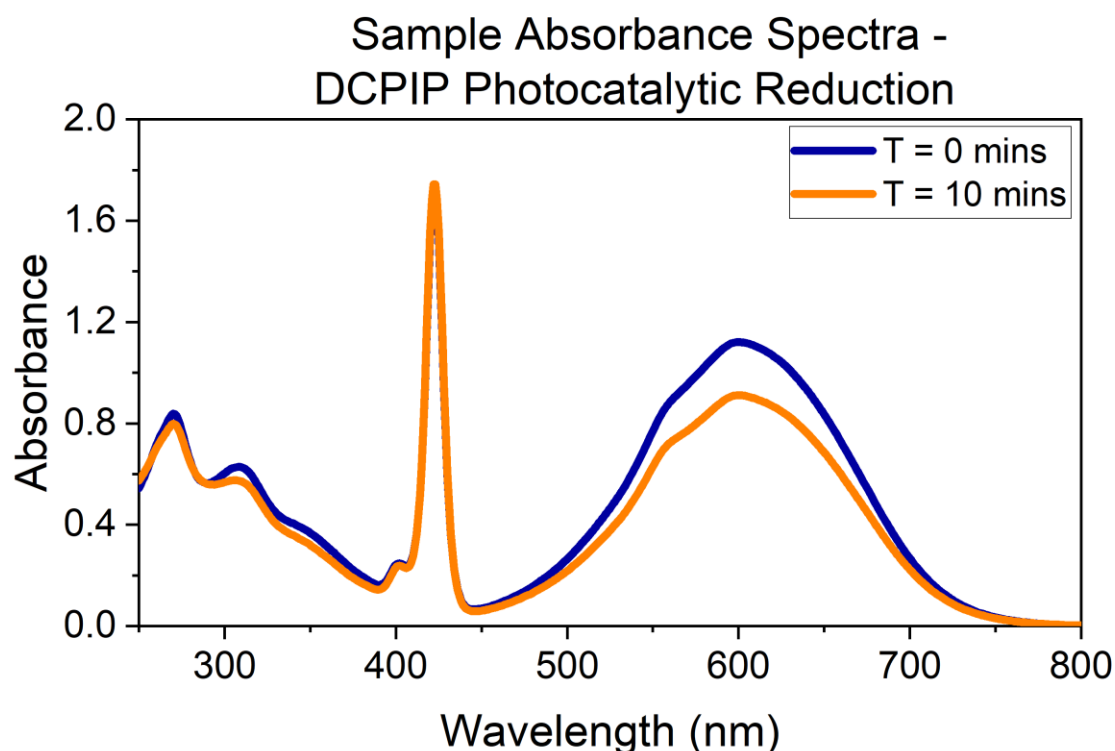

Figure 7: Absorbance spectrum of the DCPIP reaction system before and after illumination, marked as 0 mins (blue trace) and 10 mins (marked with yellow trace). The maxima for the Soret band absorbance occurs at 421 nm (in this case, for Zn^{2+}-TPPS in 2.5 µM). As is apparent from the graph above, the catalyst remains stable as per spectrophotometric recording and is not anyhow consumed during the DCPIP reduction. The latter is apparent from the decrease in absorbance for the peak centred at around 604 nm.

Since the absorbance spectra of DCPIP and the Soret-bands of any of the porphyrin molecules do not overlap, it was possible to reasonably quantify the recovery of the catalysts. In all three cases where photocatalysis was observed, there was near-complete recovery of the catalysts (Figure 7). As in the case of the methyl-red/ascorbic acid system, the turnover numbers being higher than 1 also suggest that the porphyrin complexes act as catalysts and are not consumed during the reaction.

1.3. Photoreduction of New-Methylene blue (NMB)

We intended to incorporate more model reactions to incorporate diverse functional groups, make robust conclusions about the relative photocatalytic activity of the porphyrin complexes and their stability in photocatalysis. New methylene blue (NMB, figure 8 (a)) was tested as it represents a different functional group than DCPIP and methyl red. Since its absorbance spectra does not overlap with the Soret band of the porphyrin complexes it would also allow for more accurate quantification of both dye reduction and catalyst stability.
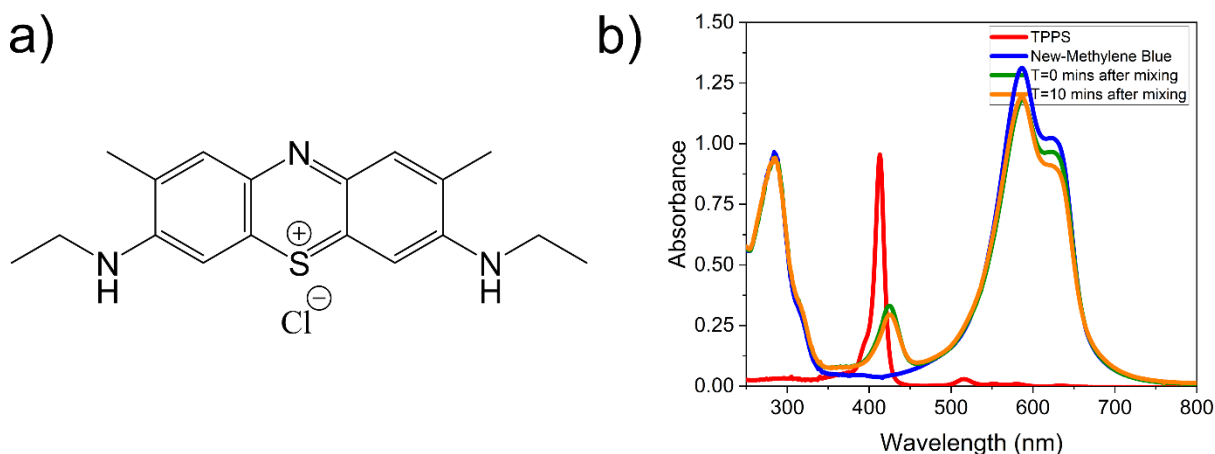

Figure 8: (a) The structure of new methylene blue used in the experiments for photoreduction. (b) The UV-Visible absorbance of 2.0 µM TPPS, 50 µM New Methylene Blue and their mixture, immediately after mixing and after 10 minutes. As is visible, there is a drop in the absorbance of TPPS and New methylene blue, although for the latter, the drop is less pronounced due to it being present in large excess (25-fold excess). Data is a representative sample, and similar observations are also seen for Zn^{2+}-TPPS.

However, on mixing, there was an instantaneous reduction in the absorbance spectra of both NMB and TPPS and the decrease continued over time (Figure 8 (b)).

Overnight, the sample showed clear visible precipitation. This is potentially due to the opposite charges (between TPPS and New Methylene Blue-N) and the tricyclic aromatic rings imparting good π-stacking.

To resolve this, we then incorporated a different water-soluble porphyrin derivative, Tetra-(N-methyl pyridyl) porphyrin (TMPyP, Figure 9 (a)) that has four positively charged methyl-pyridyl groups instead of the negatively charged benzenesulfonate groups of TPPS. This resolved the issue of precipitation.
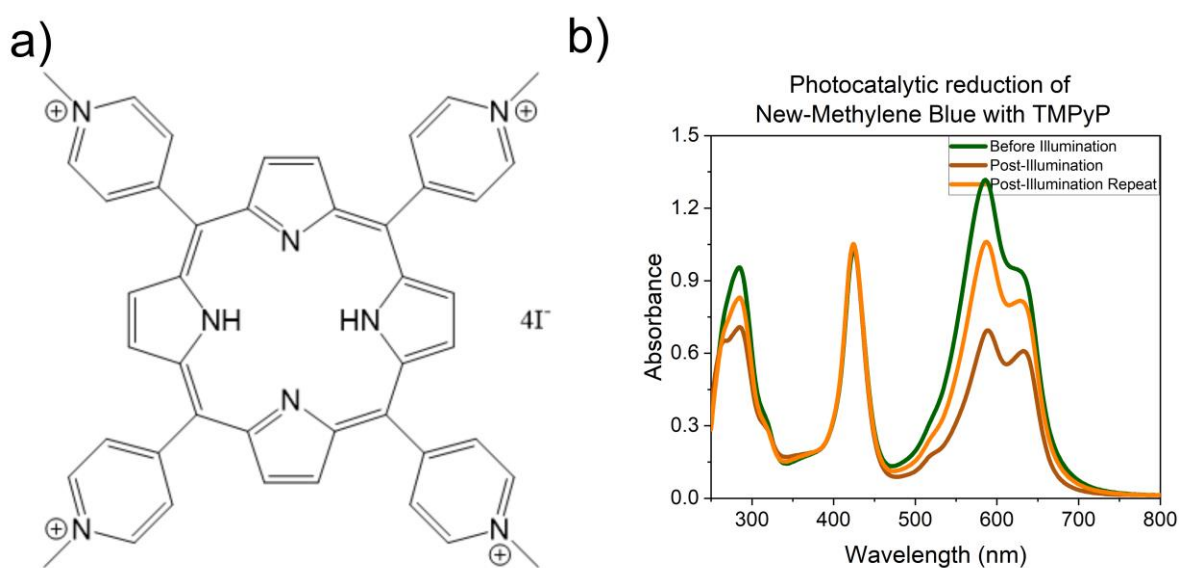

Figure 9: (a) Structure of Tetra-(N-methyl pyridyl porphyrin), abbreviated as TMPyP in the text. (b) The UV-Visible absorbance data for the photoreduction of New-methylene blue using TMPyP as the photocatalyst. Note that while the reaction does indeed progress, it has not been quantified as the reduced form re-oxidises spontaneously. Importantly, however, there is no precipitation of the substrate and catalyst. Data is a representative sample, and similar observations are also seen for Zn^{2+}-TMPyP.

With ten minutes of illumination in presence of either TMPyP and Zn^{2+}-TMPyP and TEOA as the electron donor, the deep blue coloration of NMB disappears, implying the reduction of the dye. However, the reduced form is unstable: the coloration reappears within seconds of terminating the illumination implying reoxidation of the substrate, precluding reliable quantification. These observations are also supported by the absorbance spectra, depicted in figure 9 (b). Further understanding of the system and modifications to the experimental protocols will be undertaken to ascertain the cause of the reoxidation and obtain reliable quantification.

2. Spectroscopic studies for mechanistic understanding of photocatalysis

Photocatalysis differs from normal redox catalysis because electron transfers occur from the excited states in photocatalysis. These excited states are generated when the ground state electrons absorb a photon and transition to a higher-energy level. But there is also a special requirement of stable excited states to ensure that excited state electrons are transferred to the substrate before relaxation. Diffusion limitations mandate that the lifetimes be at least in nanosecond ranges. Fluorescent states generally have lifetimes in nanosecond ranges (Figure 10).
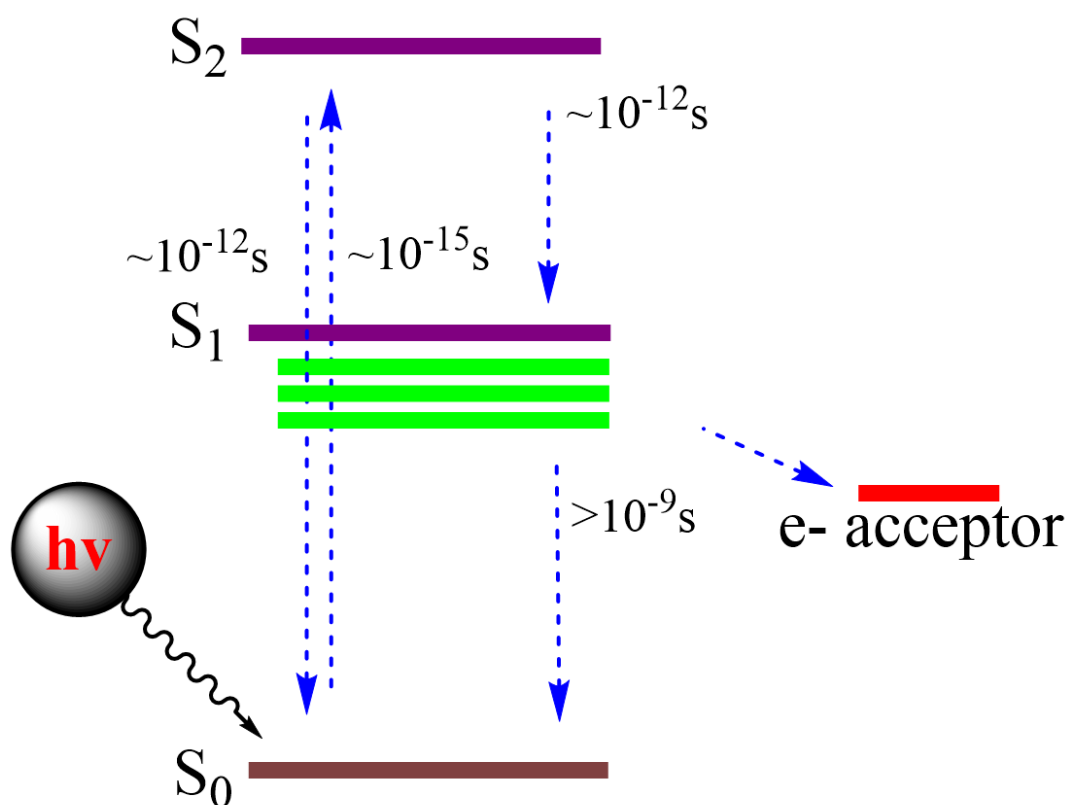

Figure 10: Jablonski Diagram representing the suggested involvement of the excited states of porphyrins in photocatalysis. The $S_2 \leftarrow S_0$ transition represents the Soret band excitation which occurs around 400-450 nm for the different complexes.

Fluorescence spectra recorded for the different complexes show that only TPPS, Mg^{2+}-TPPS and Zn^{2+}-TPPS are fluorescent active (Figure 11 (a)). Mg^{2+}-TPPS produces nearly three-fold higher fluorescence intensity compared to TPPS and five-fold higher compared to Zn^{2+}-TPPS. Furthermore, the fluorescence output followed a single-exponential decay in all cases, with lifetimes of ~10 ns for TPPS, ~6.5 ns for Mg^{2+}-TPPS and ~1.7 ns for Zn^{2+}-TPPS (Figure 11 (b)). Consistent with the hypothesis, the photocatalytic activity results from nanosecond-long fluorescent states.
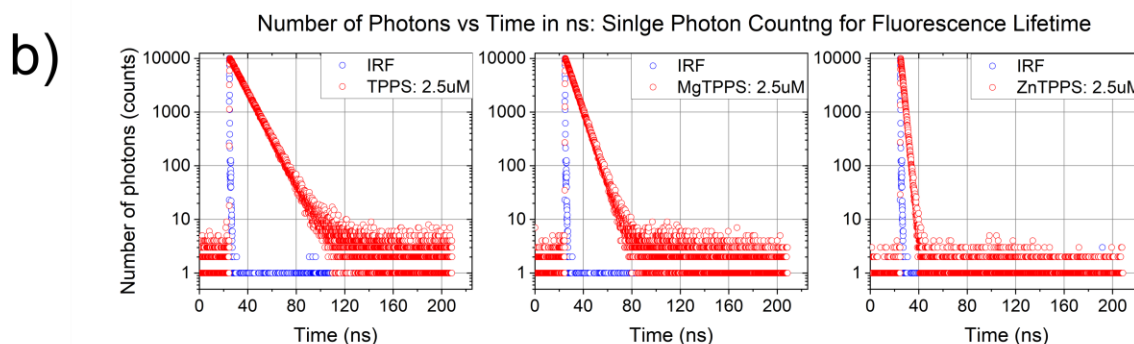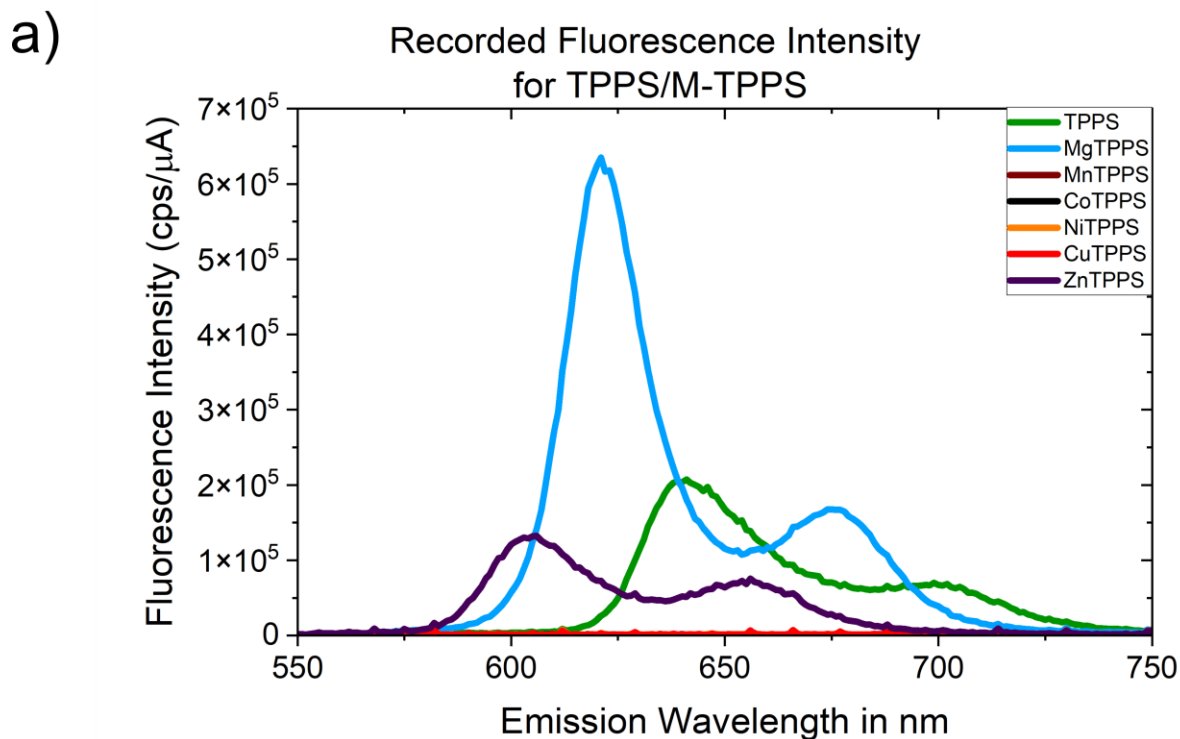
Figure 11: (a) Fluorescence Spectra for all the metalloporphyrins and the macrocycle TPPS. Each complex was excited at its respective absorbance maxima. Data average of three replicates. (b) Log plot of number of photons vs time in ns for the complexes of Mg^{2+}, Zn^{2+} and TPPS, used to record their fluorescence lifetime. A single exponential decay was found to fit best and represents the fluorescence emission from the S_1 to S_0 state.

In presence of the dyes, methyl red and DCPIP, the fluorescence spectra of the metal-complexes molecules show a reduction in intensity (Figure 12), suggesting the interaction of the porphyrin complexes in the excited state with the substrates (potentially leading to electron transfers). It is seen that the percentage quenching for a given dye is not very different in the three photocatalysts, so that the net fluorescence quenching is highest in Mg^{2+}-TPPS followed by TPPS and Zn^{2+}-TPPS. Furthermore, the quenching is consistently higher with DCPIP than with methyl red,

although the reaction progress in case of at least TPPS and Mg^{2+}-TPPS is markedly higher in the methyl red setup. It was observed that the fluorescence quenching does not occur in presence of the electron donors alone, suggesting that the excited state porphyrins cannot receive electrons from the donor without forming the radical cation first. In all cases, the structure of the excitation spectra remains unchanged in presence of the respective dyes, suggesting that the quenching is not an artefact of ground-state interactions.
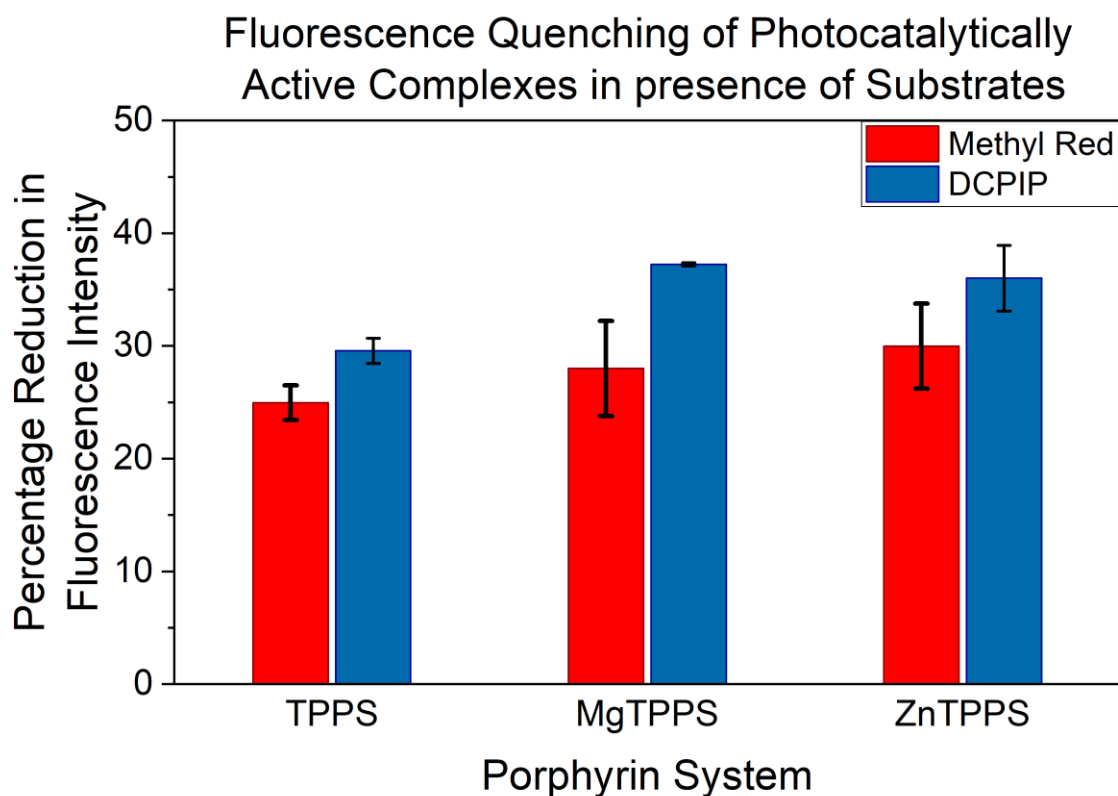

Figure 12: Percentage fluorescence quenching for TPPS, MgTPPS and ZnTPPS in presence of the dyes methyl red and DCPIP, both in 50 µM. In the former, the photocatalyst was in 500 nM concentration while in case of DCPIP, the photocatalyst was in 2.5 µM concentration. The data is average of two replicates and the error bars are standard deviations.

These trends, however, cannot be directly quantitatively correlated to the extent of reaction as is apparent from the disparity in the photocatalytic trends and the quenching patterns. The detailed reasons and the possible implications for protein evolution are discussed later. These experiments provide preliminary understandings of the photoredox mechanisms and therefore, the implications for prebiotic chemistry. Further experiments are planned to elaborate more on these details.

3. Concentration-dependence in photocatalytic efficiency

Using the DCPIP-TEOA photoredox model reaction, we next studied the effect of catalyst loading on the catalytic performance (Figure 13). With TPPS, the reaction progress increases by ~50-70% by doubling the catalyst loading, except in case of going from 1.25 µM to 2.5 µM. With Zn^{2+}-TPPS, the reaction progress increases by ~30-60 % in doubling the catalyst until 2.5 µM, but beyond ~2.5 µM of Zn^{2+}-TPPS, the reaction progress increases by only ~20 % by doubling the catalyst loading.
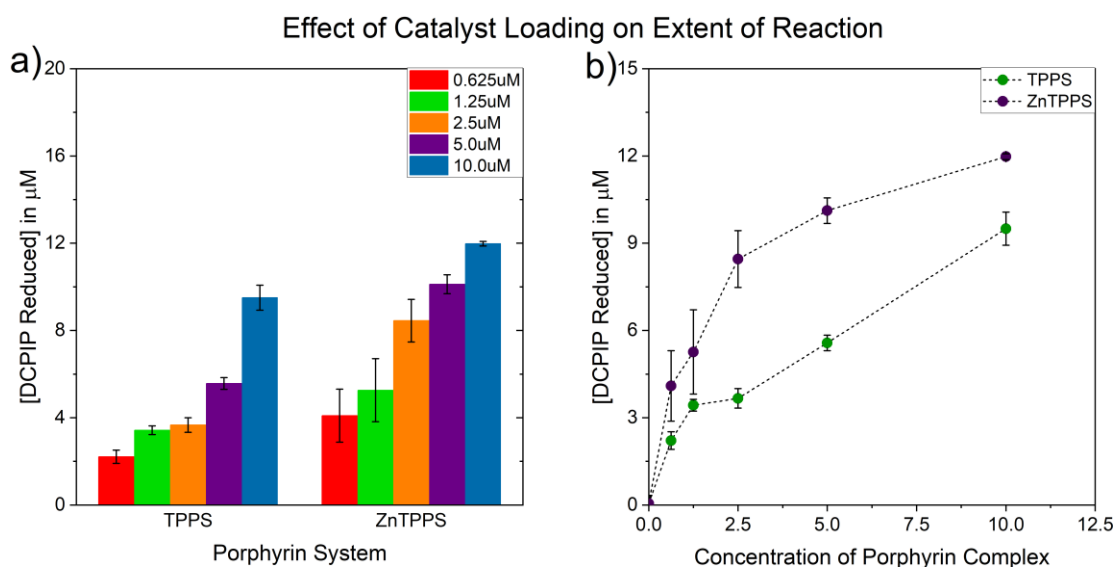

Figure 13: Photoreduction of DCPIP using TPPS and Zn^{2+}-TPPS as a function of the concentration of the catalyst shown as a bar plot in (a) and as a scatter in (b). The dotted line in (b) is not a curve fit to the data but only a visual guide to trace the data points. In both cases, the reported data is the average of two replicates and the error bars represent standard deviation.

We undertook a concentration-dependent fluorescence study to better understand the mechanism behind the non-linear change in catalytic capability.

The fluorescence maxima obtained upon excitation at the respective absorbance maxima increases up till a certain concentration and then decreases thereafter (Figure 14 a-c). In case of TPPS, the maximum occurs at 5 µM concentration while in case of Zn^{2+}-TPPS the maximum came at 7 µM concentration. While the emission spectrum remains qualitatively unchanged over the concentration range from 0.5 µM to 30 µM, the excitation spectrum splits at higher concentrations leading to the appearance of two peaks instead of one. As the concentrations increase, the maxima shift farther away from the absorbance maxima and this wavelength becomes a new minimum for the fluorescence excitation (Figure 14 d-f). The

possibility of this observation being a mere artefact of light saturation can be ruled out because saturation would likely lead to plateauing around the excitation maxima.
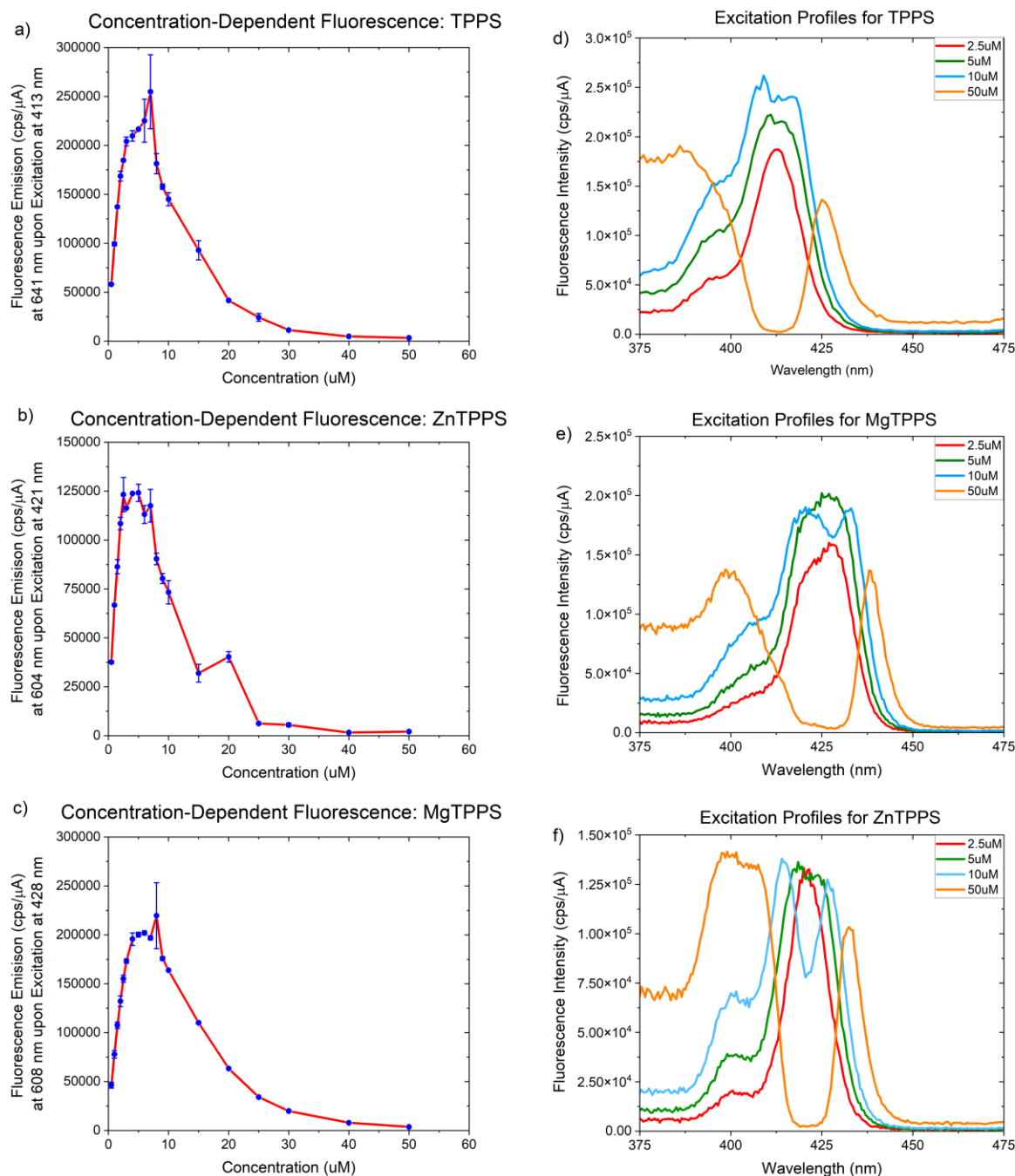
Figure 14: (a-c) The fluorescence emission recorded with the excitation maxima set at the individual absorbance maxima. Because the excitation spectra develop a progressively deeper minima at the absorbance maxima with increasing concentration, the fluorescence emission decreases steadily. (d-f) The fluorescence emission recorded with the sample excited at the excitation maxima. In all cases, the data is the average of three replicates and the error bars are standard deviations.

Discussion

Inspired by the ubiquity of porphyrin-derivatives in enzymatic machinery, the plausibility of forming such macrocycles and metal-complexes on the prebiotic earth, and specifically the role of Mg^{2+}-porphyrin complex in photosynthesis, we investigated the potential of such cofactors to have functioned as prebiotic photocatalysts. A prime goal here was to understand the selection pressure(s) that may have led to the universal role of Mg^{2+}-porphyrin complex in photosynthesis. Towards these goals, we compared the photocatalytic performance of different metal-porphyrin complexes through multiple model reactions. Thus, conclusions drawn may represent the possibility for the synthesis and photoredox of biomolecules, in general.

A definite trend we noted from the model reactions is that the porphyrin macrocycle, and its complexes with Mg^{2+} and Zn^{2+} are photocatalytically active as they are able to drive the model reactions tested, representing two distinct electron donor-acceptor pairs (and correspondingly diverse functional groups). On the other hand, the complexes of Mn^{2+}, Co^{2+}, Ni^{2+} and Cu^{2+} are photocatalytically inactive in both the reactions we tested for (and possibly in general). It is clear then, why Mn^{2+}-TPPS, Co^{2+}-TPPS, Ni^{2+}-TPPS and Cu^{2+}-TPPS cannot belong to the photocatalytic repertoire of biology. What the experiments also revealed is that at least in the absence of a supporting protein machinery, the relative photocatalytic activity among these three molecules is reaction dependent. Zn^{2+}-TPPS was the least performing out of TPPS, Mg^{2+}-TPPS and Zn^{2+}-TPPS in the photocatalytic reduction of methyl red using ascorbic acid, but was also the best performing photocatalyst in the reduction of DCPIP using TEOA. Therefore, selection for the Mg^{2+}-complex may not have readily occurred until protein evolution allowed for discriminating consistently between the complexes based on performance. In other words, protein evolution might have preceded catalytic selection in the photosynthetic machinery.

What implication does this have for prebiotic chemistry? Given the difficulty of metalating porphyrins with Mg^{2+} and the ease of metalating with Zn^{2+}, prebiotic chemistry may have had photocatalysts different from that in extant biology, perhaps employing a more diverse set of cations. Fluorescence emission should be a quantitative parameter proxy for the number of electrons available for photocatalysis.

The lack of fluorescence emission from Mn^{2+}-TPPS, Co^{2+}-TPPS, Ni^{2+}-TPPS and Cu^{2+}-TPPS explains their lack of photocatalytic activity. Further, the fluorescence emission being maximum for Mg^{2+}-TPPS among the three fluorescent-active complexes suggests that Mg^{2+}-TPPS could in principle have the maximum potential for photocatalysis. Marcus' theory of electron transfers predicts the dependence of electron transfer rates on the individual energy levels and the reorganisation energies for the donor-acceptor complex formation. This would have been particularly important in prebiotic chemistry where the photocatalyst would have directly interacted with the different substrates. Prolonged periods of evolution would have resulted in the photosynthetic machinery of extant biology, wherein downstream electron acceptors have such energy levels as to prevent back electron transfers and enhance electron transfer kinetics. We hypothesise that extant biology may be able to utilise near-complete photocatalytic capability of Mg^{2+}-porphyrin complexes projected by its fluorescence spectra.

The fluorescence quenching observed when the porphyrins interact with the substrates provides preliminary understanding of the general photocatalytic mechanism. For the substrates studied, the electron transfer from the excited state porphyrin to the acceptor is probably the first and the faster step, resulting in the radical cation state for the porphyrin. This is followed by the rate determining step, the regeneration of the ground-state porphyrin by abstracting electrons from the sacrificial electron donor. It is also possible that π-π interactions between the aromatic porphyrins and the electron acceptors facilitate easy electron transfers so that the RDS is dependent on the π-interactions between the porphyrins and the two substrates. This alternative hypothesis is easily tested by using an aromatic electron donor, such as hydroquinone. Further experiments are underway to better understand the mechanism, but the data thus far suggests that slow kinetics of catalyst regeneration leads to back-electron transfers and sub-optimal catalytic efficiency. From a prebiotic chemistry perspective then, the available repertoire of electron donors would determine the possibility of photocatalytic function for the porphyrins.

The non-linear concentration dependence of catalytic performance perhaps holds relevance for selection in the context of encapsulating mechanisms. Simpler porphyrin derivatives, which are more relevant to origins of life, are hydrophobic and are likely to sequester into hydrophobic spaces like bilayers and droplets, leading to

enhanced local concentration of the porphyrin complexes. Increased concentrations are expected to result in better photocatalysis rates. But this may not provide the same enhancement for all photocatalyst porphyrins – for e.g., Zn^{2+}-TPPS saturates in its catalytic capability at relatively lower concentrations when compared to TPPS. The fluorescence excitation spectra for all three photocatalysts shows similar changes at higher concentration, and the fluorescence saturation might be a part of the explanation as to why for Zn^{2+}-TPPS there is only a marginal increase in reaction progress despite increased catalyst loading. To the best of our knowledge, such non-linear changes to the fluorescence excitation/emission have not been reported earlier and this requires further experiments to understand the mechanism in a systematic manner.

CONCLUSION

Sunlight is known to be the major source of energy for extant life and it is intuitive that it would have been an important source of energy for prebiotic chemistry. However, sunlight is capable of driving reactions rather unselectively so that some way of channelling this energy into synthesis more selectively is necessary. Therefore, primitive bioenergetic systems would have been necessary during the origins of life to facilitate such selective synthesis of molecules relevant to the origins of life.

Our preliminary experiments suggest the functional possibility of such prebiotic photocatalytic activity using porphyrin macrocycle or metalloporphyrins. It also provides some mechanistic basis for the selection of metalloporphyrins. Further, we will aim to perform experiments involving substrates and conditions of direct relevance to the evolution of early life. Such experiments will shed light on what kind of processes could have been driven by the photocatalytic porphyrins, and the substrates in prebiotic chemistry that it could have utilised in this process.

Further understanding of the evolution of the (proto-)photosynthetic machinery and its role in the origins of life could be gleaned by evolutionary studies of the protein machinery it utilises. For example, the promiscuity of the early protein folds in binding different metalloporphyrins can give information about the possibility of different metalloporphyrins acting as photocatalysts in early life.

References

1. Alberts, B., Johnson, A., Lewis, J., Morgan, D., Raff, M., Roberts, K., & Walter, P. (2017). *Molecular Biology of the Cell*. W.W. Norton & Company. https://doi.org/10.1201/9781315735368

2. Bonfio, C., Valer, L., Scintilla, S., Shah, S., Evans, D. J., Jin, L., Szostak, J. W., Sasselov, D. D., Sutherland, J. D., & Mansy, S. S. (2017). UV-light-driven prebiotic synthesis of iron–sulfur clusters. *Nature Chemistry*, *9*(12), 1229–1234. https://doi.org/10.1038/nchem.2817

3. Branscomb, E., & Russell, M. J. (2018). Frankenstein or a Submarine Alkaline Vent: Who Is Responsible for Abiogenesis?: Part 1: What is life–that it might create itself? *BioEssays*, *40*(7). https://doi.org/10.1002/bies.201700179

4. Bromberg, Y., Aptekmann, A. A., Mahlich, Y., Cook, L., Senn, S., Miller, M., Nanda, V., Ferreiro, D. U., & Falkowski, P. G. (2022). Quantifying structural relationships of metal-binding sites suggests origins of biological electron transfer. In *Sci. Adv* (Vol. 8). https://www.science.org

5. Dagar, S., Sarkar, S., & Rajamani, S. (2022). Porphyrin in Prebiotic Catalysis: Ascertaining a Route for the Emergence of Early Metalloporphyrins**. *ChemBioChem*, *23*(8). https://doi.org/10.1002/cbic.202200013

6. Green, N. J., Xu, J., & Sutherland, J. D. (2021). Illuminating Life's Origins: UV Photochemistry in Abiotic Synthesis of Biomolecules. *Journal of the American Chemical Society*, *143*(19), 7219–7236. https://doi.org/10.1021/jacs.1c01839

7. Harel, A., Bromberg, Y., Falkowski, P. G., & Bhattacharya, D. (2014). Evolutionary history of redox metal-binding domains across the tree of life. *Proceedings of the National Academy of Sciences of the United States of America*, *111*(19), 7042–7047. https://doi.org/10.1073/pnas.1403676111

8. Herron, J. C., Scott, •, Herron, F., & Freeman, •. (2015). *Evolutionary Analysis, Global Edition*. www.pearsonglobaleditions.com

9. Miller, S. L. (1953). A Production of Amino Acids Under Possible Primitive Earth Conditions. *Science*, *117*(3046), 528–529. https://doi.org/10.1126/science.117.3046.528

10. Muchowska, K. B., Varma, S. J., & Moran, J. (2020). Nonenzymatic Metabolic Reactions and Life's Origins. In *Chemical Reviews* (Vol. 120, Issue 15, pp. 7708–7744). American Chemical Society. https://doi.org/10.1021/acs.chemrev.0c00191

11. Preiner, M., Igarashi, K., Muchowska, K. B., Yu, M., Varma, S. J., Kleinermanns, K., Nobu, M. K., Kamagata, Y., Tüysüz, H., Moran, J., & Martin, W. F. (2020). A hydrogen-dependent geochemical analogue of primordial carbon and energy metabolism. *Nature Ecology and Evolution*, *4*(4), 534–542. https://doi.org/10.1038/s41559-020-1125-6

12. Raanan, H., Pike, D. H., Moore, E. K., Falkowski, P. G., & Nanda, V. (2018). Modular origins of biological electron transfer chains. *Proceedings of the National Academy of Sciences of the United States of America*, *115*(6), 1280–1285. https://doi.org/10.1073/pnas.1714225115

13. Ritson, D. J., Mojzsis, S. J., & Sutherland, John. D. (2020). Supply of phosphate to early Earth by photogeochemistry after meteoritic weathering. *Nature Geoscience*, *13*(5), 344–348. https://doi.org/10.1038/s41561-020-0556-7

14. Ritson, D., & Sutherland, J. D. (2012). Prebiotic synthesis of simple sugars by photoredox systems chemistry. *Nature Chemistry*, *4*(11), 895–899. https://doi.org/10.1038/nchem.1467

15. Robertson, M. P., & Joyce, G. F. (2012). The origins of the RNA World. *Cold Spring Harbor Perspectives in Biology*, *4*(5), 1. https://doi.org/10.1101/cshperspect.a003608

16. Sarkar, S., Das, S., Dagar, S., Joshi, M. P., Mungi, C. V., Sawant, A. A., Patki, G. M., & Rajamani, S. (2020). Prebiological Membranes and Their Role in the Emergence of Early Cellular Life. *The Journal of Membrane Biology*, *253*(6), 589–608. https://doi.org/10.1007/s00232-020-00155-w

17. Simionescu, C. I., Simionescu, B. C., Mora, R., & Leanc, M. (1978). Porphyrin-like compounds genesis under simulated abiotic conditions. *Origins of Life*, *9*(2), 103–114. https://doi.org/10.1007/BF00931408

18. Smith, E., & Morowitz, H. J. (2016). *The Origin and Nature of Life on Earth*. Cambridge University Press. https://doi.org/10.1017/CBO9781316348772

19. Soares, A. R. M., Taniguchi, M., Chandrashaker, V., & Lindsey, J. S. (2012). Self-organization of tetrapyrrole constituents to give a photoactive protocell. *Chemical Science*, *3*(6), 1963–1974. https://doi.org/10.1039/c2sc01120d

20. Varma, S. J., Muchowska, K. B., Chatelain, P., & Moran, J. (2018). Native iron reduces CO2 to intermediates and end-products of the acetyl-CoA pathway. *Nature Ecology and Evolution*, *2*(6), 1019–1024. https://doi.org/10.1038/s41559-018-0542-2